Estimating the Effect of Crosstalk Error on Circuit Fidelity Using Noisy Intermediate-Scale Quantum Devices

Sovanmonynuth Heng, Myeongseong Go, and Youngsun Han*
Pukyong National University, Department of AI Convergence, Busan, South Korea
(Dated: February 13, 2024)

Current advancements in technology have focused the attention of the quantum computing community toward exploring the potential of near-term devices whose computing power surpasses that of classical computers in practical applications. An unresolved central question revolves around whether the inherent noise in these devices can be overcome or whether any potential quantum advantage would be limited. There is no doubt that crosstalk is one of the main sources of noise in noisy intermediate-scale quantum (NISQ) systems, and it poses a fundamental challenge to hardware designs. Crosstalk between parallel instructions can corrupt quantum states and cause incorrect program execution. In this study, we present a comprehensive analysis of the crosstalk error effect on NISQ computers. Our approach is extremely straightforward and practical for characterizing the crosstalk error of various multi-qubit devices. In particular, we combine the randomized benchmarking (RB) and simultaneous randomized benchmarking (SRB) protocol to characterize the crosstalk error from the correlation controlled-NOT (CNOT) gate. We demonstrate this protocol experimentally on 5- & 7-qubit devices. Our results demonstrate the crosstalk error model of two different IBM quantum devices over the experimental week and compare the error variation against the machine, number of qubits, quantum volume, processor, and topology of the IBM quantum devices. We then confirm the improvement in the circuit fidelity on different benchmarks by up to 3.06x via inserting an instruction barrier, as compared with an IBM quantum noisy device which offers near-optimal crosstalk mitigation in practice. Most importantly, we provide insight to ensure that the quantum operation can perform its quantum magic undisturbed. This is expected to help many quantum fields move closer to the dream of quantum supremacy and unlock new possibilities in computation.

Keywords: crosstalk error, noisy intermediate-scale quantum (NISQ), quantum device

I. INTRODUCTION

Quantum computing may be able to solve certain intractable classical problems. Companies like IBM, Google, and Rigetti have released their quantum chips with many qubits such as 433, 53, and 79 qubits, respectively [1–3]. However, these chips are classified as noisy intermediate-scale quantum (NISQ) hardware, which has less than one thousand qubits and suffers from inevitable noise. IBM Cloud now offers could-based services with 5-133 qubits, and services with more than a thousand qubits may appear in the next few years according to the IBM roadmap [4–6]. Moreover, quantum information processors (QIPs) have demonstrated 1 and 2-qubit quantum operations with error rates below the threshold required for fault-tolerant quantum computation (FTQC) [7–9]. A major obstacle to achieving similar low error rates in large and integrated quantum processors is the ability to maintain the crosstalk error [10–12].

Crosstalk can increase error rates both for individual qubits and across different qubits, in which case errors are correlated [10, 13, 14]. Such correlations make error correction difficult. Optimizing the power of quantum error correction (QEC) requires an understanding of and strict control of crosstalk errors. In addition, it is one of the major sources of noise in superconducting and also trapped-ion devices [14]. It can corrupt the qubit state when multiple quantum operations are executed simultaneously. It also has a significant impact on the quantum gate error. For instance, an increase of CNOT errors up to 3 times caused by crosstalk on IBMQ Casablanca [15], while the CNOT errors increase up to 11 times caused by crosstalk on IBMQ 20 Poughkeepsie [13]. Different protocols were proposed in [16–21] to detect and characterize crosstalk in quantum devices. After we assess crosstalk, we can introduce different mitigation techniques such as modifying simultaneous CNOT operations with high crosstalk error rate to execute sequentially while trading off an increase in depth and decoherence time [20, 22–24].

Through an analysis of real quantum computer historical calibration data from different IBM devices, we observe how device crosstalk error rates correlate between different devices and how they correlate with the ordering of the qubit connectivity. We discover some correlations in which the same correlation pair in the same device offers different crosstalk error rates than the revised of those correlation pairs, which indicates that they may share the same qubit, control, or other infrastructure. Shared infrastructure by devices could be a potential failure point for users looking for reliable execution of their programs on NISQ quantum devices. For this reason, we may prefer to avoid using devices that may share all or some of the same infrastructure. We also note that many of the calibration changes do not correlate to periods when the devices might have been offline, which represents unknown reasons for the calibration changes.

* youngsun@pknu.ac.kr

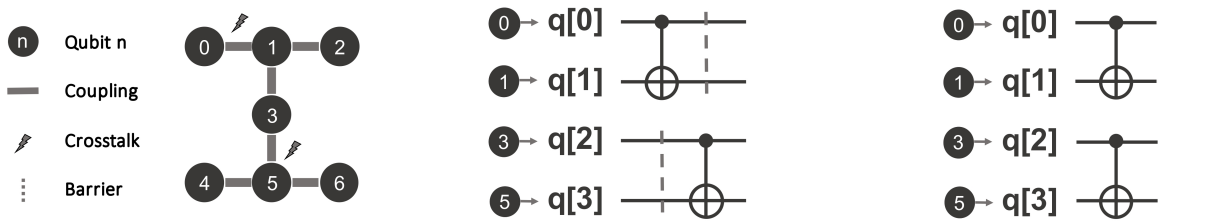

(a) IBM Nairobi 7 connectivity (b) Asynchronous CNOT execution (c) Simultaneous CNOT execution

FIG. 1: Example of the crosstalk effects characterization on IBM Nairobi 7-qubits connectivity on qubit (1,3) (marked by gray lightning) with crosstalk correlation pairing between qubit (0,1) and qubit (3,5).

However, changes to the control hardware or software have an important impact on the dependability of NISQ quantum computers.

In this work, we first introduce ways to characterize a crosstalk error using simultaneous randomized benchmarking (SRB) protocol [25]. We then model the crosstalk error model variation on each device during an experimental week. Second, we evaluate the crosstalk error model on different devices in terms of machine, number of qubits, quantum volume, processor, and topology. Finally, we insert crosstalk error pairs on different devices to show their impact on output circuit fidelity. We also demonstrate the fidelity improvement on various quantum circuit benchmarks and compare it with the results when an instruction barrier is inserted between the simultaneous crosstalk error pair. To this end, the following contributions are made in this paper.

- We validate the presence of crosstalk on two different IBM quantum devices by applying randomized benchmarking (RB) and simultaneous randomized benchmarking (SRB) protocols on several experimental simulations.
- We model and evaluate the dynamic of the crosstalk error models by comparing the error variations against the machine, number of qubits, quantum volume, processor, and topology of the IBM quantum devices.
- We demonstrate its impact on the output fidelity and the improvement of the circuit fidelity on various quantum benchmarks with up to 3.06x with the insertion of an instruction barrier.

This paper is organized as follows. Section II briefly discusses the background noise in the NISQ computers, especially crosstalk errors. Section III introduces related works on crosstalk error characterization using different techniques that motivate our study. Section IV explains our methodology for addressing crosstalk on different devices. Section V presents a detailed evaluation of the crosstalk error rate results. Section VI discusses the limitations and issues beyond current NISQ devices. We conclude our study in Section VII.

II. BACKGROUND

This section explains the primer concept of quantum bits (qubits) and quantum gates, various kinds of noise in NISQ computers, quantum device topologies, and the crosstalk error in NISQ computers.

A. Primer on Qubits and Quantum Gates

Quantum bits, or qubits $|\psi\rangle$, represent the fundamental units of quantum information in quantum computing paradigms. In stark contrast to classical bits, qubits exhibit the phenomenon of superposition, which enables them to concurrently exist in states of $|0\rangle$, or $|1\rangle$, and/or both, until they are subjected to a measurement operation [26–28]. Quantum gates, which are pivotal components in quantum computing frameworks, diverge significantly from their classical counterparts. While classical logic gates operate deterministically based on input states, quantum gates leverage the unique attributes of quantum mechanics. Quantum gates employ the principles of superposition and entanglement to execute operations on qubits, thereby enabling transformations that transcend classical logical constraints [29–31]. Prominent among quantum gates are the Hadamard gate, which is a catalyst for the generation of superposition $|\psi\rangle = \alpha|0\rangle + \beta|1\rangle$, and the CNOT gate, which facilitates qubit entanglement $|\psi\rangle = |\psi 1\rangle \otimes |\psi 2\rangle$ as shown in Figure 1b and 1c. These gates serve as quantum analogs to the classical logic gates, and they manipulate the quantum states of qubits to affect computational processes.

B. Noise in the NISQ Computer

The intricacies of noise in NISQ computers unfold across various dimensions, each contributing to the formidable challenges inherent in quantum computation. The coherence error [32] reflects the susceptibility of the qubit to environmental factors and captures the gradual loss of quantum coherence over time. Measurement errors [33] stem from detector imperfections

and signal noise to compound the challenges of obtaining precise quantum outcomes. Concurrently, two-qubit gate errors [33] arise from imperfections in the execution of quantum gates which introduce inaccuracies in state transformations. Single-qubit gate errors [33] result from imperfections in the implementation of operations on individual qubits. While decoherence noise poses a formidable threat, resulting from interactions between qubits and their external environment. Among the above types, a significant source of noise is two-qubit gates that face challenges stemming from imperfect entanglement operations namely crosstalk noise [10, 13, 14]. It exacerbates errors through unwanted interactions between neighboring qubits during quantum operations. Effectively addressing these multifaceted noise sources is crucial to improving the reliability and efficacy of NISQ computers for practical applications.

C. Quantum Device Topology

The quantum device topologies of IBM's Lima 5 [34, 35] and Nairobi 7 [36, 37] in Figure 2 represent noteworthy advancements in quantum computing architecture, specifically delineating connectivity patterns within these quantum processors. These two topologies are popular in research to address many emerging problems in practical application. Figure 2a shows IBM Lima 5 exhibiting a topological configuration characterized by five qubits and their corresponding interconnections, which reflects the intricacies of quantum entanglement and gate operations. Similarly, Figure 2b shows the IBM Nairobi 7-qubit topology, which manifests an expanded quantum processor with an intricate connectivity matrix. The connectivity within these devices is established through two-qubit gates, enabling entanglement operations between adjacent qubit pairs. The topologies, which are guided by the principles of QEC and qubit coupling, help to orchestrate quantum computations within the constraints of physical qubit relations. By elucidating these patterns of connectivity, these types of quantum device topologies contribute significantly to our understanding and optimization of quantum algorithms and error mitigation strategies in the context of emerging quantum information processing (QIP) technologies [38–41].

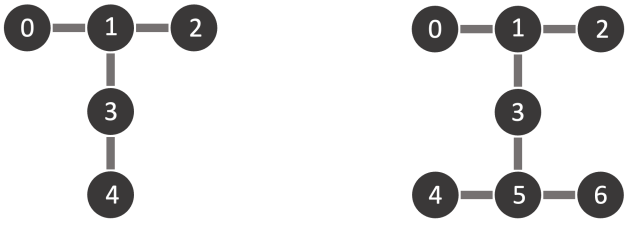

(a) IBM Lima 5 (b) IBM Nairobi 7

FIG. 2: IBM quantum devices with its connectivity.

D. Crosstalk Error in the NISQ

Crosstalk error in quantum computing refers to unwanted interaction or interference between qubits, during quantum operations [10, 13, 14]. It arises from the imperfect isolation of quantum components, and it leads to unintended effects on neighboring qubits, thereby compromising the fidelity of quantum computations. Characterizing crosstalk errors is paramount to the comprehensive assessment and improvement of quantum processors.

One prevalent technique for quantifying crosstalk errors is quantum state tomography (QST) [19], which is employed for crosstalk error characterization that involves the reconstruction of the full quantum state through a series of measurements. This technique allows for a detailed examination of the density matrix, revealing crosstalk-induced deviations from the ideal quantum states. Positive operator-valued measure (POVM) techniques [19] also contribute to crosstalk error analysis by characterizing the measurement processes. POVM enables a more nuanced understanding of measurement-induced errors and crosstalk effects, enhancing the overall comprehension of the quantum information processing landscape. Among others, the randomized benchmarking (RB) protocol [17] is the most straightforward technique as an estimated protocol in QIP. The RB protocol evaluates the average fidelity of quantum gates by subjecting them to random sequences of Clifford group gates and provides a robust measure of the global error rate. The simultaneous randomized benchmarking (SRB) protocol [18] extends this methodology to concurrently assess multiple gates of $\mathcal{E}(g_i)$ or $\mathcal{E}(g_j)$, offering insights into the collective impact of crosstalk errors on the diverse gate operations of $\mathcal{E}(g_i \mid g_j)$. If the crosstalk error exists between them, the relation between independent and correlated errors should comply with $\mathcal{E}(g_i \mid g_j) > \mathcal{E}(g_i)$ or $\mathcal{E}(g_j \mid g_i) > \mathcal{E}(g_j)$.

To calculate the rate of the correlated error to independent error as an indicator of the crosstalk effect on CNOT pairs, we used the following equation 1.

$$r(g_i \mid g_j) = \mathcal{E}(g_i \mid g_j) / \mathcal{E}(g_i) \tag{1}$$

These RB and SRB protocols can be used in as many iterations as possible to address the most scalable and accurate CNOT error rate because CNOT errors vary with each calibration on different devices[42–44].

III. RELATED WORK AND MOTIVATION

Crosstalk error has been studied extensively in recent years with its opportunity in terms of mitigation [16–18, 45]. Some studies have characterized, modeled, and analyzed crosstalk errors by applying the benefit of the simultaneous randomized benchmarking (SRB) protocol [17, 21, 37, 46]. Moreover, the techniques used in studies [11, 16, 47, 48] to detect or characterize crosstalk

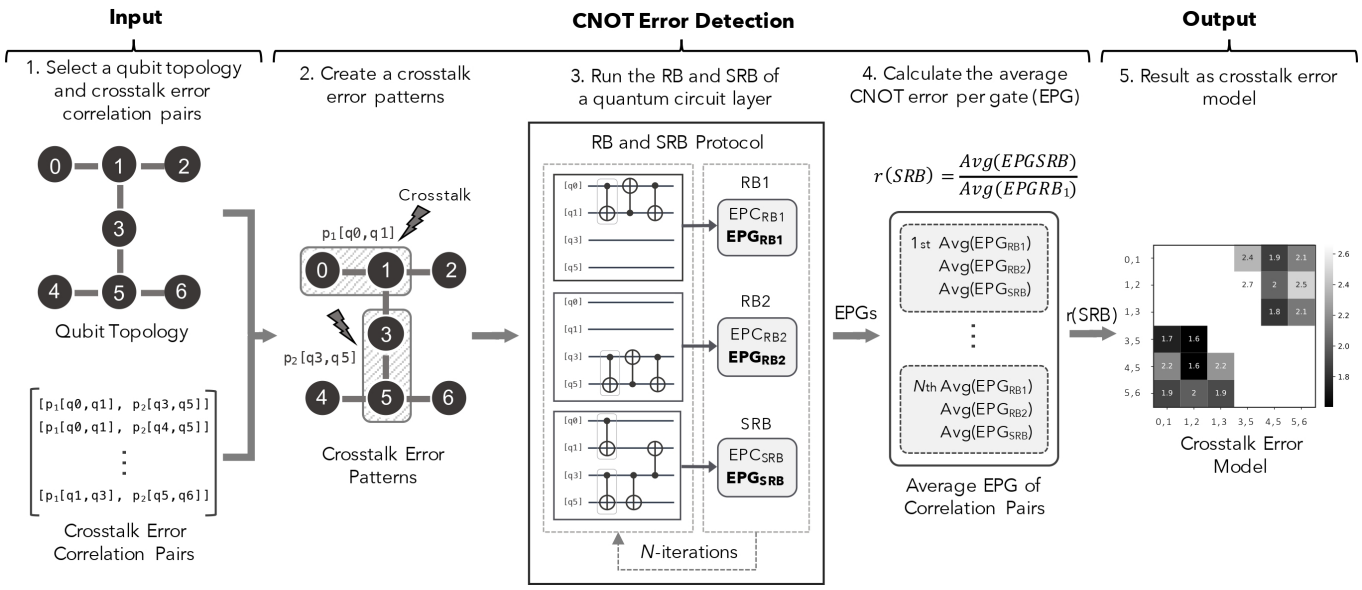

FIG. 3: Schematic implementation of the crosstalk error characterization using randomized benchmarking (RB) and simultaneous randomized benchmarking (SRB) protocol. These protocols can be subdivided into three parts, depicted within the different curly brackets for input, CNOT error detection, and output. The crosstalk error model can be addressed by detecting each CNOT error pair with a randomly generated RB and SRB protocol from the crosstalk error patterns to obtain each Error Per Clifford (EPC) and Error Per Gate (EPG).

error involve quantum tomography methods such as gate set tomography, idle tomography, process tensor tomography, and parallel tomography. However, some methods based on process tomography involve a process matrix having significant computational complexity to measure crosstalk errors, and it is difficult to distinguish between crosstalk errors reliably [18]. However, [19] employed the quantum mechanics physiology of the positive operator-valued measure (POVM) to quantify crosstalk error and define the nature of the error. Similarly, [10] was measured and characterized crosstalk by focusing on its impact on the gate performance in quantum systems, particularly in the context of simultaneous gate operations on superconducting qubits.

However, most of the aforementioned studies [16–21, 45, 46] were conducted ultimately to apply their proposed mitigation technique. As a result of this simplicity, these methods may not comprehensively address the intricate dynamics of crosstalk errors and their impact on different devices. In addition, [16–21] are out-of-date data since crosstalk error is a very emerging type of error that requires up-to-date data to address its effect from real machines with detailed analysis. In light of this study [19], it becomes evident that a single qubit crosstalk error is too small to address or interfere with the quantum computation. The trade-off between the number of qubits, resource consumption, the difficulty of characterization, and the crosstalk effect. The problem we want to address in our study is not about the mitigation technique; the most challenging first task is to realize how much error rate on each pair and how much error rate we will face if we do not mitigate it. Moreover, we believe that not all crosstalk error rates on different devices of multiple qubits are created equal and there are many different factors to take into account which we will demonstrate in this study.

IV. METHODOLOGY

In this section, we will discuss the overall protocol we used to characterize the crosstalk error for different devices and the detailed technique used for crosstalk detection and implementation with the RB & SRB protocols.

A. Overall Protocol

To characterize the effect of the crosstalk error model on quantum devices, we follow the RB and SRB protocols which we segment into three distinct phases namely input, CNOT error detection, and output. These components are delineated for discussion within the protocol, as illustrated in Figure 3.

To address the crosstalk error, we first select the qubit topology of the quantum device such as IBM Lima or IBM Nairobi, as shown in Figure 2 or another quantum device as needed. We also analyze the pattern based on the selected topology to address the crosstalk error correlation pairs as input to another step in the protocol. To analyze the pattern of crosstalk error for each topology, Khadirsharbiyani et al. [49] stated that if two qubits do

not have simultaneously running CNOTs, no crosstalk occurs. Hence, we use these crosstalk rules of no duplicate qubits in our experiment. For instance, Figure 2b shows IBM Nairobi with a 7-qubit topology. The pattern of the crosstalk error pairing with [0, 1] would be [0, 1] and [3, 5], [0, 1] and [4, 5], [0, 1] and [5, 6], and so on. The pattern that does not have a crosstalk error would be [0, 1] and [0, 1] or [0, 1] and [1, 2], since these pairs are redundant for qubit (0 and 1), and qubit (1), respectively. By following this rule for all crosstalk error correlation pairs, we derive the crosstalk error pattern of IBM Nairobi.

Then, the quantum circuit layer for the RB and SRB protocols is generated using the input as a crosstalk error pattern. Each iteration of CNOT error detection involves the use of two RB and one SRB quantum circuit layer. When two RB quantum circuit layers are employed, one layer corresponds to the first pair of qubits and the other layer corresponds to the second pair of qubits. The simulation randomly selects two qubits from several available qubits for the Clifford group gates, which results in only two qubits being used. Similarly, the SRB quantum circuit layer requires the random selection of four qubits for the Clifford group gates. Subsequently, the Error Per Gate (EPG) for the CNOT gate errors per iteration is calculated. The experimental setup can accommodate as many iterations as are feasible to enhance accuracy. Upon the completion of each iteration, both the RB and SRB circuit layers yield their respective EPG values. To calculate the EPG, the initial step involves computing the average Error Per Clifford (EPC) for either the RB or SRB circuit layers. In the RB experiment, the Clifford group gates and their inverse gate sequences are randomly sampled, and the average EPC is then derived using the $pref$ parameter (where $pref$corresponds to a reference parameter with d = 2 for a single qubit) [50]. Subsequently, the EPG for the CNOT gate in each iteration is calculated. Previous studies [51, 52] have indicated that each circuit layer decomposition has on average 1.5 CNOT gates per Clifford group gate and reported as an upper bound on the EPG as roughly equivalent to EPC/1.5.

Using the EPG results from each iteration, we can finally calculate the average output of the EPG of the CNOT errors for the two RB and the single SRB quantum circuit layers, denoted as $Avg(EPG_{RB1})$, $Avg(EPG_{RB2})$, and $Avg(EPG_{SRB})$, respectively. The $Avg(EPG_{RB1})$ and $Avg(EPG_{SRB})$ values are used to determine the crosstalk error rate $r(SRB)$ and assess the dynamic occurrence of crosstalk error on specific error correlation pairs within the topology. If the summation of $Avg(EPG_{RB1})$ and $Avg(EPG_{RB2})$ over $Avg(EPG_{RB1})$ is found to be less than $Avg(EPG_{SRB})$ alone, then it can be inferred that there is no presence of crosstalk. Otherwise, a crosstalk error occurs and its rate is $r(SRB)$ which is equivalent to $Avg(EPG_{SRB})$ over $Avg(EPG_{RB1})$.

ALGORITHM 1: CNOT Error Detection

Data:
bg: basic gates,
nQ: number of qubits,
nS: number of seeds,
nC: number of Clifford group gates,
$P1$: crosstalk correlation pair 1,
$P2$: crosstalk correlation pair 2
Result:
EPG_{RB1}: Randomized Benchmarking Pair 1,
EPG_{RB2}: Randomized Benchmarking Pair 2,
EPG_{SRB}: Simultaneous RB between Pair 1 & 2

```
for pair1 ∈ P1 do
    for pair2 ∈ P2 do
        for r ∈ 3 do
            if r == 0 then
                nQ = 2;
                pattern = [pair1];
                EPC_RB1 = (bg, nQ, nS, nC, pattern);
                EPG_RB1 = EPC_RB1 / 1.5;
            else if r == 1 then
                nQ = 2;
                pattern = [pair2];
                EPC_RB2 = (bg, nQ, nS, nC, pattern);
                EPG_RB2 = EPC_RB2 / 1.5;
            else
                nQ = 4;
                pattern = [pair1, pair2];
                EPC_SRB = (bg, nQ, nS, nC, pattern);
                EPG_SRB = EPC_SRB / 1.5;
            end
        end
    end
end
```

B. Crosstalk Error Characterization

To characterize the crosstalk error in IBM quantum devices, we first must address each CNOT error correlation pair for the crosstalk error pair. Algorithm 1 describes the operation of the RB and SRB protocols to detect each CNOT error on different IBM quantum devices. The algorithm begins by deciding the necessary input components such as basic gates (bs), number of qubits (nQ), number of seeds (nS), number of Clifford group gates (nC), crosstalk correlation pair 1 (P1), and crosstalk correlation pair 2 (P2), which are generated according to the connectivity of the selected quantum device or topology. After completing this process, we use an experimental quantum circuit layer of RB and SRB to calibrate the EPC and EPG. Then, we are able to analyze whether or not the crosstalk error occurs on that specific correlated pair of qubits. For the first iteration of the CNOT error detection, we first address the two RB circuit layers in two separate 2-qubit crosstalk correlation pairs ([P1] and [P2]) and one SRB circuit layer between the 4-qubit crosstalk correlation pairs ([P1] with [P2]) simultaneously. If we want to address the RB circuit layer of q_i and q_j, we use only two qubits ($nQ = 2$) that are

randomly generated for the circuit layer based on the pattern of pair1 or pair2 to find the EPG_{RB1} or EPG_{RB2}. Otherwise, we will use four randomly generated qubits ($nQ = 4$) to find the EPG_{SRB} between the pattern of pair1 and pair2 simultaneously. Finally, the algorithm returns the output components of EPG_{RB1} and EPG_{RB2} for the RB circuit layer and of the EPG_{SRB} for the SRB circuit layer, depending on the input components of the topology. These outputs are used to observe whether or not there is a crosstalk error occurs and how severe it is for that specific pair of crosstalk correlation pairs. For example, if the EPG_{SRB} is greater than the summation of EPG_{RB1} and EPG_{RB2} over EPG_{RB1}, then there is a crosstalk error rate on top of the CNOT error.

V. EVALUATION

In this section, we discuss our experimental setup and evaluate the RB and SRB protocols by presenting our crosstalk error model, daily variation in the crosstalk error, comparing the dynamic of the crosstalk error model, and illustrating the impact of crosstalk error on several benchmark circuits using two IBM quantum devices.

A. Experimental Setup

To facilitate our evaluation, we present an experimental setup for addressing the crosstalk error simulation.

Backend: We select two different IBM quantum devices namely IBM Fake LimaV2 with 5 qubits and IBM Fake NairobiV2 with 7 qubits as the backend for the entire experiment depends on the type of machine, number of qubits, quantum volume, processor, and topology of the IBM quantum devices.

Experimental Circuit: We use random circuits for randomized benchmarking (RB) with a default of 1024 shots and n number of qubits based on the device's basic gates. In each experimental circuit layer, we randomly combined 150 Clifford group gates in the circuit layer together and ran them for 5 iterations (5 seeds). Each iteration includes 8 subcircuits, so we have 40 subcircuits to execute and calculate the average number of errors per gate (EPG). Many qubit errors, particularly crosstalk errors, are not apparent in low-width circuit layers; thus, studying low-width circuit layers is insufficient. Hence, our goal is to scale the RB and SRB to quantify the average error in high-width circuit layer sets.

Baselines: A circuit with no simultaneous CNOT is used as the baseline for comparison with the number of CNOT insertions simultaneously into the circuit.

Benchmark: We select a small-scale circuit as a benchmark that fits in with our two IBM quantum devices to validate the fidelity, namely grover_n2, toffoli_n3, cat_state_n4, and Ipn_n5.

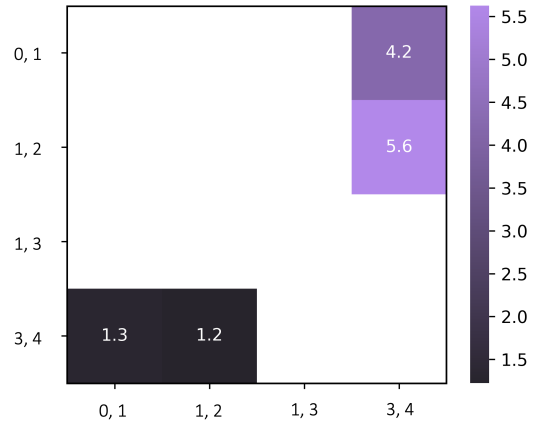

(a) Average crosstalk error rate for IBM Lima

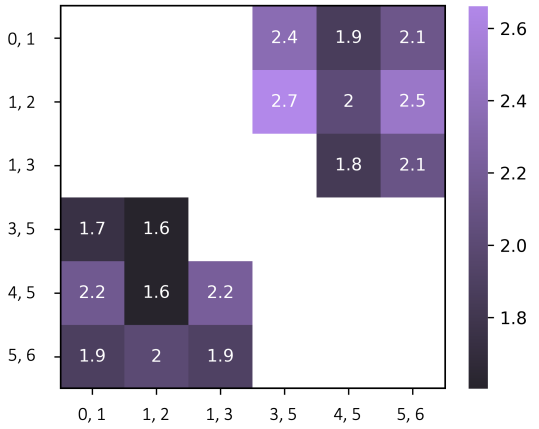

(b) Average crosstalk error rate for IBM Nairobi

FIG. 4: Average crosstalk error rate model for different IBM quantum devices. The x-axis and y-axis represent the pairwise correlation between qubit pair 1 and qubit pair 2, respectively. A lighter purple color indicates a higher crosstalk error rate on both devices.

B. Crosstalk Error Models

To illustrate the presence of crosstalk error, we conducted an experiment using two different IBM quantum devices. For a fair result, Figure 4 presents the average crosstalk error characterization on each of the IBM quantum devices over 5 consecutive days. A correlation pair with no color is a correlation pair with no crosstalk because it contains duplicate qubits, such as [0, 1] and [0, 1] or [1, 2] and [0, 1], whereas the color purple indicates a correlation pair with crosstalk error based on its variation mode.

Figure 4a shows the average crosstalk error rate for IBM Lima 5. From these results, we can see that the crosstalk correlation pair with the minor error pair is [3, 4] and [1, 2] because it is darker in color and the most severe is [1, 2], and [3, 4] because it is lighter in color. In addition, Figure 4b shows the average crosstalk error rate for IBM Nairobi 7. It shows more crosstalk correlation

pairs because it uses 7 qubits in this topology. The minor error pairs are [3, 5] and [1, 2] and [4, 5] and [1, 2], whereas the most severe is the pair [1, 2] and [3, 5].

This result shows that the crosstalk correlation pair varies depending on the pair selected for the operation. Even the same pair with the reverse of the qubit pair can also create a very different crosstalk error rate. Notably, the ascending number of qubit orders usually got a higher crosstalk effect on the operation. For example, [1, 2] and [3, 4] are more severe than [3, 4] and [1, 2] on IBM Lima 5, and [1, 2] and [3, 5] are more severe than [3, 5] and [1, 2] on IBM Nairobi 7. Hence, both figures show that the upper-right correlation pair is lighter in purple, which indicates the severity of the crosstalk error pair. In contrast, the bottom left is a darker purple, which indicates a minor crosstalk error pair.

C. Daily Variation in Crosstalk Error

To illustrate the daily variation in the crosstalk error, we present the daily variation in the crosstalk error rate for 5 consecutive days starting from December 4, 2023 to December 8, 2023 using two different IBM quantum devices. Figure 5 shows the daily variation in the crosstalk error rate on IBM Lima 5 and IBM Nairobi 7. This variation indicates the consistency for the same device even though we performed experiments on different days. The consistency refers to the level of the crosstalk correlation pairs behaved among other pairs. The line on all pairs (both devices) seems to go up and down; this variation corresponds to the updated calibration data provided by the IBM cloud services.

Figure 5a shows the daily variation in the crosstalk error rate for IBM Lima. The severe crosstalk correlation pair of [1, 2] and [3, 4] is colored in the black solid line with the circle markers. The minor crosstalk correlation pair of [0, 1] and [3, 4] is colored in the black dotted line with the star markers. The daily variation in the crosstalk error rate varies up to 4.66x on average (1.2 to 5.6) for IBM Lima.

Figure 5b shows the daily variation in the crosstalk error rate for IBM Nairobi. The severe crosstalk correlation pair of [1, 2] and [3, 5] is a black solid line with circle markers. The minor crosstalk correlation pair of [1, 3] and [4, 5]] is colored in the black solid line with square markers. Among others, we observe that the crosstalk correlation pairs of [0, 1] and [5, 6], which are shown as the black solid line with the triangle markers are the most consistent from December 4, 2023 to December 7, 2023. The daily variation in the crosstalk error rate varies up to 1.68x on average (1.6 to 2.7) for IBM Nairobi.

This daily variation indicates that not all crosstalk correlation pairs behave quite the same way on every single day of the experiment. However, it does indicate that the severe pairs are still severe and the minor pairs are still minor pairs. We note that the variation for IBM Nairobi 7 is extremely low compared with the IBM Lima 5. The reason for this is that the IBM Nairobi 7 has greater quantum volume (QV) than the IBM Lima 5 in which the QV is the metric that measures the capabilities and error rates of quantum devices.

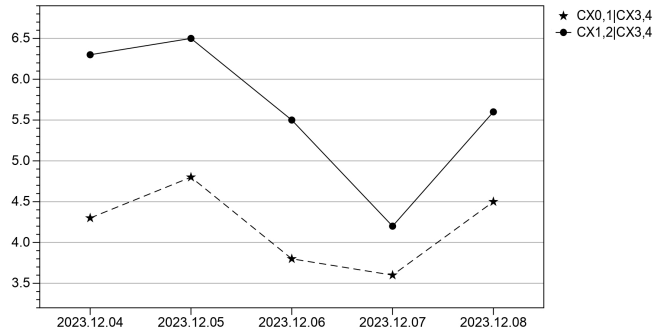

(a) Daily variation of crosstalk error rate for IBM Lima

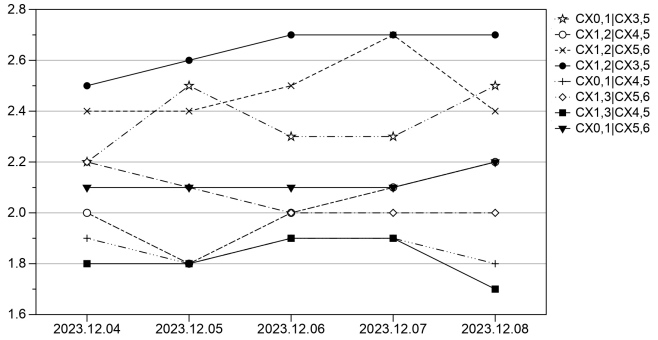

(b) Daily variation of crosstalk error rate for IBM Nairobi

FIG. 5: Daily variation in crosstalk error rate for two different IBM quantum devices. The x-axis represents the five consecutive days of experimentation, and the y-axis represents the crosstalk error rate. Each line with a marker represents a distinguished individual crosstalk correlation pair on the devices.

D. Crosstalk Error Model Comparison

Table I shows the detailed crosstalk error model for two different IBM quantum devices in terms of machine, number of qubits (#Qubit), quantum volume (QV), processor, crosstalk mode, and topology.

Within the IBM Lima architecture, a Falcon r4T configuration contains five qubits carefully arranged in a T topology connectivity. Contrary to expectations, the crosstalk error model exhibited by these arrangements surpasses that observed for the IBM Nairobi device. It is noteworthy that despite the modest number of qubits (just five) and a quantum volume of eight, the Falcon r4T configuration on IBM Lima experiences a significantly more pronounced crosstalk error. The severity of the crosstalk error on this machine is approximately 2.5x greater than that encountered on the IBM Nairobi.

Although the new Falcon r5.1H IBM Nairobi processor boasts a configuration of seven qubits, a standout attribute is its remarkable reduction in crosstalk errors. Adding to its technical capability, this processor is ingeniously arranged as an H processor type with higher levels of connectivity. The driving force behind this notable achievement lies in the quantum volume, which reaches an impressive 32. This substantial increase in quantum volume translates into a significant enhancement of error rates, particularly for crosstalk errors.

After we analyze the comparison between the IBM Lima 5 and IBM Nairobi 7 devices, it is evident that the selection of a specific device holds significant importance in the execution of various operations, notably in terms of quantum error mitigation (QEM) and quantum error correction (QEC). This comparison emphasizes the critical role that the choice of a quantum device plays in ensuring the efficacy and success of operations that involve error mitigation and correction within the quantum computing paradigm.

E. Impact of Crosstalk Error on Circuit Fidelity

Finally, we evaluate the crosstalk error for the most severe IBM Nairobi to determine its effect on the circuit fidelity. We choose four benchmarks from [53] like grover_n2, toffoli_n3, cat_state_n4, and Ipn_n5 with the different numbers of qubits and gates per benchmark. We prepare all experimental benchmarks at optimization level 0, which is no optimization for the simulation to determine the real effect of crosstalk error. The baseline is no simultaneous CNOTs (no crosstalk) with the experimental benchmarks.

Figure 6 shows the impact of the crosstalk error of the Probability of Success Trails (PST) on the small-scale benchmarks of 2-5 qubits on the IBM Nairobi 7-qubits device. PST is the real system success probability of the number of trails with the correct measurement result divided by the total number of trails when executing on the real simulation. The probability of obtaining the right output state decreases with an increase in simultaneous CNOTs due to the inserted crosstalk error. Inserting the crosstalk error decreases the PST by 1.85x on average (up to 3.06x) based on the noise model of the tested pair. This experimental result is based on the highest crosstalk error pair in the crosstalk error model for the IBM Nairobi.

In the case of grover_n1, the fidelity decreases by 44.05% compared with the non-crosstalk case. When we compare the presence of a barrier with no barrier in terms of output fidelity, the fidelity is improved by 2.06x. In the best case of toffoli_n3, the fidelity decreases by 30.54% and improves by 3.06x when a barrier is inserted. In the worst case, such as for cat_state_n4, the fidelity decreases by 48.35% compared with the non-crosstalk case. In our comparison in terms of output fidelity and circuit depth with and without a barrier, the fidelity improves by 1.87x. With Ipn_n5, the fidelity decreases by 40.21% with an improvement of 2.3x after the barrier is inserted.

As we can see from the figure above, the insertion of a barrier results in an improvement in output fidelity up to almost the same level as that of no crosstalk errors. Consequently, this work may lead to a greater interest in QEM techniques in the future.

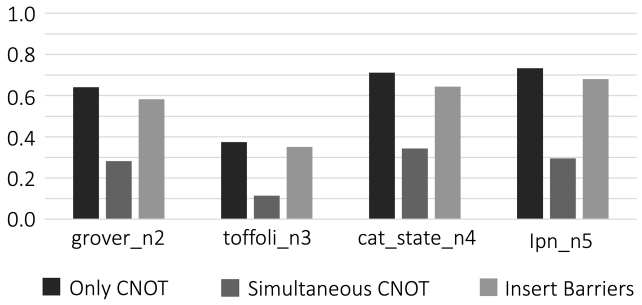

FIG. 6: Probability of Success Trails (PST) for four benchmarks under different conditions with only CNOT gate, with simultaneous CNOT gates, and with barriers along with simultaneous CNOT gates.

VI. DISCUSSION AND LIMITATIONS

A recent trend in QEM techniques [54] is to exploit greater potential from the crosstalk error with a greater number of mitigation opportunities. Unlike innovations that are mostly driven by the underlying technologies, our study takes the first profound direction which is to enable a deeper understanding of the crosstalk error model for different devices by leveraging the RB and SRB protocols. Relatively little attention has been paid to this approach for two main reasons: 1) it is exceedingly difficult to extract useful information from a large number of circuit and gate sequences, which is the accurate level at which most operations today operate, and 2) the scalability of the protocol on all different devices, which is an effective static analysis of a protocol, becomes quite difficult as the size of the operation matrix grows exponentially with the number of qubits. We believe that these are two critical yet difficult problems in the understanding of crosstalk error characteristics because they prevent the quantum operation from performing correctly.

Limited Value on a Realistic System: As the data are limited on realistic systems, specific details about the current state of IBM's quantum devices and their performance with real-world data may not be available to all researchers. The progress made by and specifications for quantum devices is continuously evolving as research and development in quantum computing advance. To obtain the most accurate and up-to-date information about IBM's quantum devices, including any limited crosstalk error from real systems, we used a fake device that mimics a real system. Additionally, due to the expensive runtime

Machine	#Qubits	QV	Processors	Crosstalk Mode	EPG_{RB1}	EPG_{RB2}	EPG_{SRB}	Topology
IBM Lima	5	8	Falcon r4T	Minor	0.004	0.026	1.2	
				Medium	0.007	0.023	3.4	
				Severe	0.010	0.037	5.6	
IBM Nairobi	7	32	Falcon r5.11H	Minor	0.006	0.006	1.6	
				Medium	0.0075	0.009	2.15	
				Severe	0.009	0.012	2.7	

TABLE I: Characteristics of IBM quantum devices used in our study, IBM Lima and IBM Nairobi. Each device has a different number of qubits (#Qubit), quantum volume (QV), processor, crosstalk mode, Error Per Gate of RB and SRB (EPG_{RB1}, EPG_{RB2}, and EPG_{SRB}), and topology.

cost and the limits of crosstalk metric within the RB and SRB protocols on a real system, a fake device is preferable for this study.

Noise Beyond the NISQ Systems: In systems other than NISQ systems, the noise problem in quantum computing becomes more severe as researchers develop quantum components that are more fault-tolerant. QEC is paramount, and it demands additional qubits and computational resources. The challenges include mitigating decoherence and environmental interactions, reducing error rates, ensuring scalability while managing noise, improving quantum hardware, and refining noise models for accurate characterization. Strategies such as hybrid quantum-classical approaches may serve to address these challenges, as the field focuses on building robust, scalable quantum computers that are capable of handling errors effectively and enabling practical quantum information processing. However, our study experiments with the current NISQ devices, which have a different way of handling errors to explore more in the practical QIP.

Trade-off between Fidelity and Depth: Although the fidelity is enhanced because of the insertion barrier, the increase in circuit depth is not negligible. Fidelity is crucial to reliable quantum computation, and it represents the accuracy of quantum operations. However, the depth of the quantum circuit and the number of sequential quantum operations may be compromised to reduce the crosstalk error. This trade-off arises because mitigation techniques to counter crosstalk can lead to increased computational overhead and decreased depth. Striking the right balance is essential, as sacrificing too much depth may undermine the computational advantage offered by quantum systems. Researchers are exploring innovative techniques and error-mitigation strategies that maintain an equilibrium between fidelity and depth to ensure the efficient functioning of quantum circuits while effectively suppressing the disruptive effects of crosstalk.

Mitigation Opportunity: Mitigating crosstalk errors provides a valuable opportunity to enhance the robustness and reliability of quantum information processing. By identifying and implementing effective mitigation strategies, researchers can significantly minimize the impact of crosstalk, thereby improving the overall performance of quantum circuits. Opportunities for mitigation crosstalk include the development of error correction codes, optimized control mechanisms, and advanced calibration techniques. Moreover, leveraging QEC methods can help counteract the undesirable effects of crosstalk by preserving the integrity of quantum states during computation. As quantum computing technologies advance, exploring novel mitigation opportunities will be crucial to unlocking the full potential of quantum systems and ensuring their viability in practical applications in the future to bridge between NISQ and FTQC.

VII. CONCLUSION AND OUTLOOK

In this work, we leverage the RB and SRB protocols to quantify the effect of crosstalk errors on the NISQ computers. The RB and SRB protocols enable the accurate estimation of crosstalk errors by measuring average gate performance by running sequences of random Clifford group gates that should return the qubits to their initial state simultaneously. This provides an estimation of the error for the two-qubit crosstalk correlation error pair on different quantum devices in a systematic manner. We provide comprehensive error information for each device as a crosstalk error model, its daily variation, and a comparison between the two devices. Additionally, we evaluate the impact of crosstalk error on several small-scale benchmarks to determine the improvements in circuit fidelity brought about by the insertion of an instruction barrier. Our use of RB and SRB protocols could be extended to different backends and devices by configuring the topology correlation of the crosstalk error pairs. Our work confirms that these protocols can address the crosstalk error model on different devices and a straightforward estimation protocol in a more effective, scalable, and better reconfigurable method. Future work on analytically bounding the number of iterations could demonstrate the performance of this method against well-known characterization techniques. We believe that the results explored in this study would promote future work in the direction of exploring the crosstalk error model in the context of producing a better quantum algorithm.

ACKNOWLEDGMENTS

This research was partly supported by Quantum Computing based on Quantum Advantage challenge research (RS-2023-00257994) through the National Research Foundation of Korea (NRF) funded by the Korean government (MSIT) and Institute for Information & communications Technology Planning & Evaluation (IITP) grant funded by the Korea government (MSIT) (No. 2020-0-00014, A Technology Development of Quantum OS for Fault-tolerant Logical Qubit Computing Environment).

[1] C. Q. Choi, Ibm's quantum leap: The company will take quantum tech past the 1,000-qubit mark in 2023, IEEE Spectrum **60**, 46 (2023).

[2] F. Arute, K. Arya, R. Babbush, D. Bacon, J. C. Bardin, R. Barends, R. Biswas, S. Boixo, F. G. Brandao, D. A. Buell, *et al.*, Quantum supremacy using a programmable superconducting processor, Nature **574**, 505 (2019).

[3] E. J. Gustafson, A. C. Li, A. Khan, A. Kahn, J. Kim, D. M. Kurkcuoglu, M. S. Alam, P. P. Orth, A. Rahmani, and T. Iadecola, *Preparing quantum many-body scar states on quantum computers*, Tech. Rep. (Fermi National Accelerator Lab.(FNAL), Batavia, IL (United States), 2023).

[4] H. Riel, Quantum computing technology, in *2021 IEEE International Electron Devices Meeting (IEDM)* (IEEE, 2021) pp. 1–3.

[5] C. Xu and J. Szefer, Long-term analysis of the dependability of cloud-based nisq quantum computers, in *Proceedings of the 18th International Conference on Availability, Reliability and Security* (2023) pp. 1–6.

[6] J. Alvarado-Valiente, J. Romero-Álvarez, E. Moguel, J. García-Alonso, and J. M. Murillo, Technological diversity of quantum computing providers: a comparative study and a proposal for api gateway integration, Software Quality Journal , 1 (2023).

[7] A. Noiri, K. Takeda, T. Nakajima, T. Kobayashi, A. Sammak, G. Scappucci, and S. Tarucha, Fast universal quantum gate above the fault-tolerance threshold in silicon, Nature **601**, 338 (2022).

[8] A. Hashim, S. Seritan, T. Proctor, K. Rudinger, N. Goss, R. K. Naik, J. M. Kreikebaum, D. I. Santiago, and I. Siddiqi, Benchmarking quantum logic operations relative to thresholds for fault tolerance, npj Quantum Information **9**, 109 (2023).

[9] L. Postler, S. Heuβen, I. Pogorelov, M. Rispler, T. Feldker, M. Meth, C. D. Marciniak, R. Stricker, M. Ringbauer, R. Blatt, *et al.*, Demonstration of fault-tolerant universal quantum gate operations, Nature **605**, 675 (2022).

[10] P. Zhao, K. Linghu, Z. Li, P. Xu, R. Wang, G. Xue, Y. Jin, and H. Yu, Quantum crosstalk analysis for simultaneous gate operations on superconducting qubits, PRX quantum **3**, 020301 (2022).

[11] A. Ash-Saki, M. Alam, and S. Ghosh, Analysis of crosstalk in nisq devices and security implications in multi-programming regime, in *Proceedings of the ACM/IEEE International Symposium on Low Power Electronics and Design* (2020) pp. 25–30.

[12] S. Niu and A. Todri-Sanial, Multi-programming mechanism on near-term quantum computing, in *Quantum Computing: Circuits, Systems, Automation and Applications* (Springer, 2023) pp. 19–54.

[13] P. Murali, D. C. McKay, M. Martonosi, and A. Javadi-Abhari, Software mitigation of crosstalk on noisy intermediate-scale quantum computers, in *Proceedings of the Twenty-Fifth International Conference on Architectural Support for Programming Languages and Operating Systems* (2020) pp. 1001–1016.

[14] J. Gaebler, C. Baldwin, S. Moses, J. Dreiling, C. Figgatt, M. Foss-Feig, D. Hayes, and J. Pino, Suppression of midcircuit measurement crosstalk errors with micromotion, Physical Review A **104**, 062440 (2021).

[15] D. C. McKay, A. W. Cross, C. J. Wood, and J. M. Gambetta, Correlated randomized benchmarking, arXiv preprint arXiv:2003.02354 (2020).

[16] M. Sarovar, T. Proctor, K. Rudinger, K. Young, E. Nielsen, and R. Blume-Kohout, Detecting crosstalk errors in quantum information processors, Quantum **4**, 321 (2020).

[17] S. Niu and A. Todri-Sanial, Analyzing crosstalk error in the nisq era, in *2021 IEEE Computer Society Annual Symposium on VLSI (ISVLSI)* (IEEE, 2021) pp. 428–430.

[18] K. Rudinger, C. W. Hogle, R. K. Naik, A. Hashim, D. Lobser, D. I. Santiago, M. D. Grace, E. Nielsen, T. Proctor, S. Seritan, *et al.*, Experimental characterization of crosstalk errors with simultaneous gate set tomography, PRX Quantum **2**, 040338 (2021).

[19] S. Seo and J. Bae, Measurement crosstalk errors in cloud-based quantum computing, IEEE Internet Computing **26**, 26 (2021).

[20] Y. Ding, P. Gokhale, S. F. Lin, R. Rines, T. Propson, and F. T. Chong, Systematic crosstalk mitigation for superconducting qubits via frequency-aware compilation, in *2020 53rd Annual IEEE/ACM International Symposium on Microarchitecture (MICRO)* (IEEE, 2020) pp. 201–214.

[21] A. Ash-Saki, M. Alam, and S. Ghosh, Experimental characterization, modeling, and analysis of crosstalk in a quantum computer, IEEE Transactions on Quantum Engineering **1**, 1 (2020).

[22] R. A. M. Razif, S. M. M. Maharum, A. H. Hasani, and Z. Mansor, Mitigation techniques for crosstalk in ics, in *IOP Conference Series: Materials Science and Engineering*, Vol. 701 (IOP Publishing, 2019) p. 012037.

[23] A. Winick, J. J. Wallman, and J. Emerson, Simulating and mitigating crosstalk, Physical review letters **126**, 230502 (2021).

[24] L. Xie, J. Zhai, and W. Zheng, Mitigating crosstalk in quantum computers through commutativity-based instruction reordering, in *2021 58th ACM/IEEE Design Automation Conference (DAC)* (IEEE, 2021) pp. 445–450.

[25] J. M. Gambetta, A. D. Córcoles, S. T. Merkel, B. R. Johnson, J. A. Smolin, J. M. Chow, C. A. Ryan, C. Rigetti, S. Poletto, T. A. Ohki, M. B. Ketchen, and M. Steffen, Characterization of addressability by simultaneous randomized benchmarking, Phys. Rev. Lett. **109**, 240504 (2012).

[26] S. T. Marella and H. S. K. Parisa, Introduction to quantum computing, Quantum Computing and Communications (2020).

[27] F. de Lima Marquezino, R. Portugal, and C. Lavor, *A primer on quantum computing* (Springer, 2019).

[28] J. D. Hidary and J. D. Hidary, *Quantum computing: an applied approach*, Vol. 1 (Springer, 2019).

[29] M. J. Renner and Č. Brukner, Computational advantage from a quantum superposition of qubit gate orders, Physical Review Letters **128**, 230503 (2022).

[30] P. A. Ivanov and N. V. Vitanov, Two-qubit quantum gate and entanglement protected by circulant symmetry, Scientific Reports **10**, 5030 (2020).

[31] S. Mummadi and B. Rudra, Fundamentals of quantum computation and basic quantum gates, in *Handbook of Research on Quantum Computing for Smart Environments* (IGI Global, 2023) pp. 1–24.

[32] A. Krasnok, P. Dhakal, A. Fedorov, P. Frigola, M. Kelly, and S. Kutsaev, Superconducting microwave cavities and qubits for quantum information systems, Appl Phys Rev **11** (2024).

[33] M. Zheng, A. Li, T. Terlaky, and X. Yang, A bayesian approach for characterizing and mitigating gate and measurement errors, ACM Transactions on Quantum Computing **4**, 1 (2023).

[34] R. Selvarajan, V. Dixit, X. Cui, T. S. Humble, and S. Kais, Prime factorization using quantum variational imaginary time evolution, Scientific reports **11**, 20835 (2021).

[35] V. Russo, A. Mari, N. Shammah, R. LaRose, and W. J. Zeng, Testing platform-independent quantum error mitigation on noisy quantum computers, IEEE Transactions on Quantum Engineering (2023).

[36] D. Konar, E. Gelenbe, S. Bhandary, A. D. Sarma, and A. Cangi, Random quantum neural networks (rqnn) for noisy image recognition, arXiv preprint arXiv:2203.01764 (2022).

[37] S. Niu and A. Todri-Sanial, Enabling multi-programming mechanism for quantum computing in the nisq era, Quantum **7**, 925 (2023).

[38] D. Singh, S. Jakhodia, and B. Jajodia, Experimental evaluation of adder circuits on ibm qx hardware, in *Inventive Computation and Information Technologies: Proceedings of ICICIT 2021* (Springer, 2022) pp. 333–347.

[39] B. Baheri, D. Chen, B. Fang, S. A. Stein, V. Chaudhary, Y. Mao, S. Xu, A. Li, and Q. Guan, Tqea: Temporal quantum error analysis, in *2021 51st Annual IEEE/IFIP International Conference on Dependable Systems and Networks-Supplemental Volume (DSN-S)* (IEEE, 2021) pp. 65–67.

[40] H. Yetis and M. Karakoes, Investigation of noise effects for different quantum computing architectures in ibm-q at nisq level, in *2021 25th International Conference on Information Technology (IT)* (IEEE, 2021) pp. 1–4.

[41] S. Martina, L. Buffoni, S. Gherardini, and F. Caruso, Learning the noise fingerprint of quantum devices, Quantum Machine Intelligence **4**, 8 (2022).

[42] J. Helsen, I. Roth, E. Onorati, A. H. Werner, and J. Eisert, General framework for randomized benchmarking, PRX Quantum **3**, 020357 (2022).

[43] J. Hines, M. Lu, R. K. Naik, A. Hashim, J.-L. Ville, B. Mitchell, J. M. Kriekebaum, D. I. Santiago, S. Seritan, E. Nielsen, *et al.*, Demonstrating scalable randomized benchmarking of universal gate sets, Physical Review X **13**, 041030 (2023).

[44] A. R. Mills, C. R. Guinn, M. J. Gullans, A. J. Sigillito, M. M. Feldman, E. Nielsen, and J. R. Petta, Two-qubit silicon quantum processor with operation fidelity exceeding 99%, Science Advances **8**, eabn5130 (2022).

[45] R. Liu, Z. Guan, X. Cheng, P. Zhu, and S. Feng, Suppression of crosstalk in quantum computers based on instruction exchange rules and duration, in *Journal of Physics: Conference Series*, Vol. 2524 (IOP Publishing, 2023) p. 012026.

[46] M. Ibrahim, N. T. Bronn, and G. T. Byrd, Crosstalk-based parameterized quantum circuit approximation, arXiv preprint arXiv:2305.04172 (2023).

[47] G. A. White, F. A. Pollock, L. C. Hollenberg, K. Modi, and C. D. Hill, Non-markovian quantum process tomography, PRX Quantum **3**, 020344 (2022).

[48] L. Pereira, J. J. García-Ripoll, and T. Ramos, Parallel tomography of quantum non-demolition measurements in multi-qubit devices, npj Quantum Information **9**, 22 (2023).

[49] S. Khadirsharbiyani, M. Sadeghi, M. E. Zarch, J. Kotra, and M. T. Kandemir, Trim: crosstalk-aware qubit mapping for multiprogrammed quantum systems, in *2023 IEEE International Conference on Quantum Software (QSW)* (IEEE, 2023) pp. 138–148.

[50] Z. Li, P. Liu, P. Zhao, Z. Mi, H. Xu, X. Liang, T. Su, W. Sun, G. Xue, J.-N. Zhang, *et al.*, Error per single-qubit gate below 10^{-4} in a superconducting qubit, arXiv preprint arXiv:2302.08690 (2023).

[51] K. Wei, E. Magesan, I. Lauer, S. Srinivasan, D. Bogorin, S. Carnevale, G. Keefe, Y. Kim, D. Klaus, W. Landers, *et al.*, Hamiltonian engineering with multicolor drives for fast entangling gates and quantum crosstalk cancellation, Physical Review Letters **129**, 060501 (2022).

[52] A. Finck, S. Carnevale, D. Klaus, C. Scerbo, J. Blair, T. McConkey, C. Kurter, A. Carniol, G. Keefe, M. Kumph, *et al.*, Suppressed crosstalk between two-junction superconducting qubits with mode-selective exchange coupling, Physical Review Applied **16**, 054041 (2021).

[53] A. Li, S. Stein, S. Krishnamoorthy, and J. Ang, Qasmbench: A low-level quantum benchmark suite for nisq evaluation and simulation, ACM Transactions on Quantum Computing **4**, 10.1145/3550488 (2023).

[54] J. Sun, X. Yuan, T. Tsunoda, V. Vedral, S. C. Benjamin, and S. Endo, Mitigating realistic noise in practical noisy intermediate-scale quantum devices, Phys. Rev. Appl. **15**, 034026 (2021).